Parallel spring stages with flexures of micrometric cross sections

Simon Henein, Stefano Bottinelli, Reymond Clavel

Simon Henein, Stefano Bottinelli, Reymond Clavel, "Parallel spring stages with flexures of micrometric cross sections," Proc. SPIE 3202, Microrobotics and Microsystem Fabrication, (1 January 1998); doi: 10.1117/12.298039

SPIE.

Event: Intelligent Systems and Advanced Manufacturing, 1997, Pittsburgh, PA, United States

Parallel spring stages with flexures of micrometric cross-sections

Simon Henein[a], Stefano Bottinelli and Reymond Clavel

EPFL : Swiss Federal Institute of Technology of Lausanne
DMT-IMT EPFL, CH-1015 Lausanne Switzerland

ABSTRACT

This paper describes a detailed study of the behaviour of the parallel spring stage having four circular flexure hinges of very thin cross-sections (from 22μm to 50μm) manufactured by wire Electro-Discharge Machining.

The state of the art recalls the abundant literature published on the parallel leaf spring stage, and presents the few articles found dealing with the parallel spring stages.

The theoretical modelling for the calculation of the linear stiffness of the parallel spring stage is described.

The starting point of the discussion is the observation that the theoretical model which is valid when applied to stages of large dimensions produces large errors when applied to wire-EDM machined flexures of very thin cross-sections.

As an explanation of this observation, a hypothesis is put forward : on the surface of each neck a thin layer affected by the EDM process is not playing any mechanical role in the bending of the flexure and the thickness of this layer (called "neutral zone") is related to the roughness of the surface.

The experimental results (measurements made on 18 stages made of steel and aluminium) show that the hypothesis is true to a large extent but that roughness is probably not the only factor affecting the neutral zone. The "white layer" and the microstructural homogeneity of the material used could also be determinant.

Keywords : flexure, notch hinge pivot, parallel spring stage, wire electro-discharge machining, surface roughness, high precision robotics

1. INTRODUCTION

1.1 Flexible structures for microrobots of ever higher precision

In the fields of semiconductors, opto-electronic interconnection and microsystems in general, the demand for precise positioning has grown along with the increasing miniaturisation of the structures which are to be handled or tested. The automatic manufacturing and assembly of these devices, which allows mass production at very low costs, require micromanipulators with ever higher precision[1]. In many cases an inappropriate mechanical structure for a robot can be an insurmountable limiting factor to its precision. For example backlash or friction can hardly be overcome by sensors or controllers. An efficient approach to this problem is to use a new concept of structures specially dedicated to microrobots : these structures are free from friction, backlash and wear at their articulations through the use of *flexible bearings* replacing the traditional rolling or plain bearings.

1.2 Parallel spring stage

One of the most simple and common of these flexible structures is the *parallel leaf spring stage* (fig. 1.a) which provides a curvilinear translation. This mechanism has been thoroughly described and widely used, as we will see in the state of the art. More recently, the development of machining processes and especially the increasing utilisation of wire electro-discharge machining has led to the use of an other type of linear mechanism using four necked down flexure hinges (notch hinges) instead of leaf springs (fig. 1.c). It is this latter mechanism, simply called *parallel spring stage,* which will be the subject matter of this paper.

[a] Email : simon.henein@epfl.ch ; http://dmtwww.epfl.ch/imt; Telephone : ++41 21 693 58 53; Fax : ++ 41 21 693 58 59

1.3 Wire electro-discharge machining of small flexures

As it has been clearly noticed[2], the main limitation of flexures is their short range of motion. It is due to the stresses in the flexures which must be kept below the yield stress of the material. The need for long strokes requires flexures of ever thinner cross-sections. *Wire electro-discharge machining*[3] (wire-EDM) has shown to be one of the most suited manufacturing processes for this purpose, for it allows the manufacturing of necked down sections of various shapes with thinknesses thinner than 50µm, geometrical tolerances of the order of ±1µm and low surface roughnesses. Moreover, the machined pieces are not subject to any mechanical stresses which could alter their geometry, and materials with very high elastic limits[a] can easily be machined.

1.4 The need for a more accurate model for small flexures

At this micrometric scale, flexures have a behaviour which differs from what could be predicted by the classical analytical models. Our study is an attempt to understand how wire-EDM machined flexures with cross-sections thinner than 50µm behave. The candidate we have chosen to be our object of study is the parallel spring stage because its linear motion makes its stiffness easy to measure. Moreover, it is simple and representative of other varieties of flexures. Hence, we expect to be able to generalise the observations drawn from these experiments to other more complex flexible structures.

1.5 Plan of the paper

The state of the art will recall the abundant literature published on the parallel leaf spring, showing how often this linear flexible device can be soundly used. Then it will present the few articles dealing with the parallel spring stages.

The chapter on the theoretical modelling will discuss two models for the calculation of the linear stiffness of the parallel spring stage found in literature and the model we have developed on our own.

Then the wire electro-discharge machining of the parallel spring stages and the stiffness measurements procedure will be described.

Finally a comparison between the experimental results and the theoretical models will allow us to see what are the limits of these models when applied to flexures of micrometric cross-sections : it appears that parallel spring stages having necked down sections with thinknesses ranging from 25µm to 50µm have lower stiffnesses than predicted by classical analytical models. We will try to provide explanations to this phenomenon, and will show that a model which takes into account the roughness of the flexure's surface better fits the experimental results.

2. STATE OF THE ART

The parallel spring stage is a descendant of the parallel leaf spring stage. Hence it is interesting to quickly review the literature published on the latter before studying the former.

2.1 The parallel leaf spring stage

Descriptions of the parallel leaf spring stage can already be found at the beginning of this century[4]. Since then, the behaviour of this structure has been closely studied (straightness of motion[5,6,7], pitching errors[8]) . Numerous variants of it are described[9,10,11], the most common of which is the compound parallel leaf spring stage.

The parallel leaf spring stage is now slowly being replaced by the monolithic parallel spring stage which fulfils the same function but which does not require the difficult assembly and tuning[12] steps of the former, and hence is more predictable[13].

2.2 The parallel spring stage (with four notch hinges)

This new type of linear mechanism has been used for many micro-positioning applications such as monomode optics[14,15], x-ray interferometric scanning[16,17,18] and LSI photomasks linewidth measurements[19]. But the theoretical studies of this stage[2,13,20] are much less numerous than that of the former. We will discuss them in detail in the coming chapter.

---

[a] The search for long motion ranges calls for materials with high elastic limits (like hardened steels) which are often difficult to machine by traditional metal cutting.

What is new in our research is that we are studying flexures of extremely small cross-sections (20µm to 50µm) which have the advantage of having the longest motion ranges, and that we are trying to take the manufacturing process (wire-EDM) into account in our theoretical model.

3. THEORETICAL MODELLING

In this chapter two models for the calculation of the linear stiffness of the parallel spring stage found in the literature are presented. Then a third model we have developed from our own is described. Finally the three models are compared.

3.1 Parameters defining the parallel spring stage

E : Young's modulus of the material, r : radius of the notches, e : thickness at the middle of the joints, b : width of the joints, l : length of the arms from neck to neck.

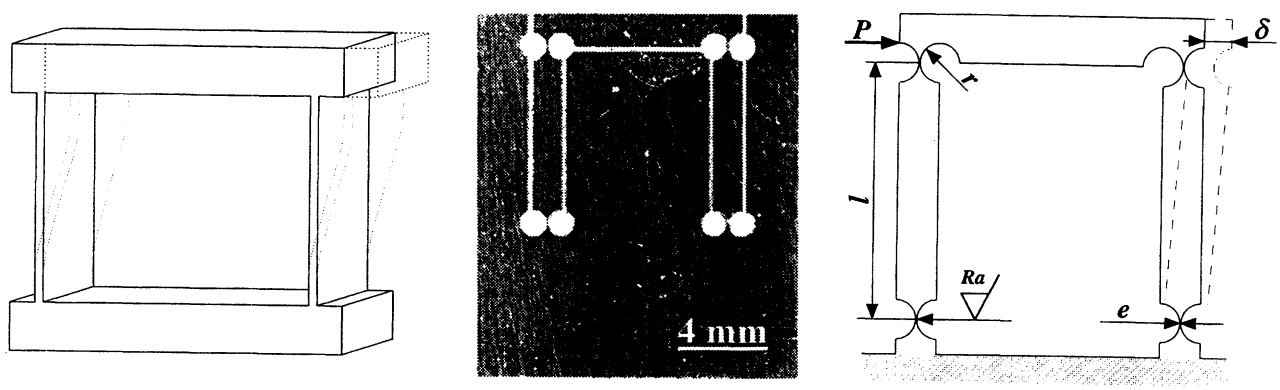

a. b. c.

Figure 1 : a. Parallel leaf spring stage.
b. Photography of one of the small parallel spring stages we machined.
c. Geometrical parameters defining the parallel spring stage. The linear stiffness is : $K = P / \delta$.

3.2 Model 1

Smith[13] gives a formula for the calculation of the linear stiffness of the parallel spring stage : $\boxed{K_1 = \frac{E.I_{zz}}{c.r.l^2}}$ where c is a factor determined from finite elements analysis of the circular flexure hinge : $c = 0.565\frac{e}{r} + 0.166$ and $I_{zz} = \frac{b.e^3}{12}$.

3.3 Model 2

Paros[20] gives a formula for the angular stiffness of the circular flexure hinge : $K_\alpha = \frac{2.E.b.e^{\frac{5}{2}}}{9.\pi.r^{\frac{1}{2}}}$.

Smith[2] uses the latter term to establish a formula of the linear stiffness of the parallel spring stage : he considers the circular flexure hinge as an ideal pivot whose centre of rotation is located in the middle of the neck and whose angular stiffness is K_α. For a drive force P applied at a height midway between the moving and the fixed platform of the parallel spring stage, a pure bending moment $M = \frac{P.l}{4}$ plus a force $F = \frac{P}{2}$ act on each joint. In accordance with the hypothesis that the pivots are ideal, the force F has no effect on the joints and it is solely M which will bend them of an angle $\alpha = \frac{M}{K_\alpha}$. Thus, for small angles α the linear stiffness of the stage is : $\boxed{K_2 = \frac{4.K_\alpha}{l^2}}$

3.4 Model 3

In reality, the circular flexure hinge is not an ideal pivot but rather a beam of varying cross-sectional area. Therefore we must consider not only the pure bending moment, but also the nonuniform bending moment due to the forces acting on the joint, to calculate its deflection (the bending moment changes as we move along the axis of the joint). In this case the deflection is more complex than a simple rotation about a fixed point located in the middle of the joint. To take this into account we first calculated the effect of a pure bending moment on a notch hinge. Then we calculated the effect of a bending force applied to the tip of a notch hinge. Finally, by decomposing the loads on each joint of a parallel spring stage in terms of pure bending and forces applied to the tip of the joints we established a formula for the linear stiffness of the parallel spring stage. This process is described below.

In practice, the drive force P is usually applied on the moving platform (like on fig. 1.c) rather than midway between the fixed and the moving platform. In this case an axial loading (tension or compression) appears on the joints. This axial loading of the joints causes pitching errors of the movement of the platform [5,8] (referred to as "cantilever bending of the parallel spring stage") but does not affect its linear stiffness. Since in this study we are concerned only with the linear stiffness of the stages, we have established a model which takes into account the nonuniform bending of the joints but not their axial loading.

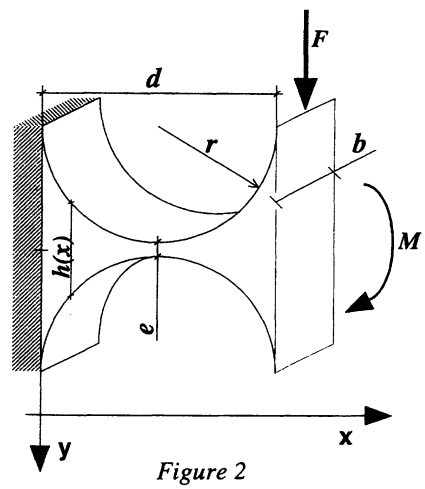

Figure 2

Stiffnesses of a single joint :

The height of the joint is : $h(x) = 2.r + e - 2.\sqrt{r^2 - (r-x)^2}$

The moment of inertia of the cross-section of the joint is : $I(x) = \frac{b.(h(x))^3}{12}$

If $y(x)$ is the elastic line of the deformed joint, $y'(x) = \frac{dy}{dx}$ and $y''(x) = \frac{d^2y}{dx^2}$, then we have[21] : $y''(x) = \frac{-M(x)}{E.I(x)}$.

For a pure bending moment M applied on the joint (see fig. 2 for orientation) $M(x) = -M$.

The angular stiffness is $K_{\alpha M} = \frac{M}{y'(d)}$ and we define $K_{fM} = \frac{M}{y(d)}$.

For a force F applied to the joint's end (fig. 2) $M(x) = -F(d-x)$.

The linear stiffness is $K_{fF} = \frac{F}{y(d)}$ and we define $K_{\alpha F} = \frac{F}{y'(d)}$.

These equations have been solved numerically by computer[a].

Linear stiffness of a parallel spring stage :

Using the stiffnesses calculated above for a single joint, we have derived the linear stiffness of a stage having four of these joints : $\boxed{K_3 = 2.\left(\frac{L^2}{2.K_{\alpha M}} - \frac{L}{K_{\alpha F}} - \frac{L}{K_{fM}} + \frac{2}{K_{fF}}\right)^{-1}}$ where L is the total length of the legs : $L = l + 2.r$.

3.5 Comparison between the three models

It is essential for our study to choose the best theoretical model available. For this purpose we have compared the three models when applied to stages of our dimensions (fig. 3) : r = 0.6125mm, l = 8mm, b = 5.5mm, E = 2.1 10^{11}N/m^2 and e is ranging between 20µm and 50µm.

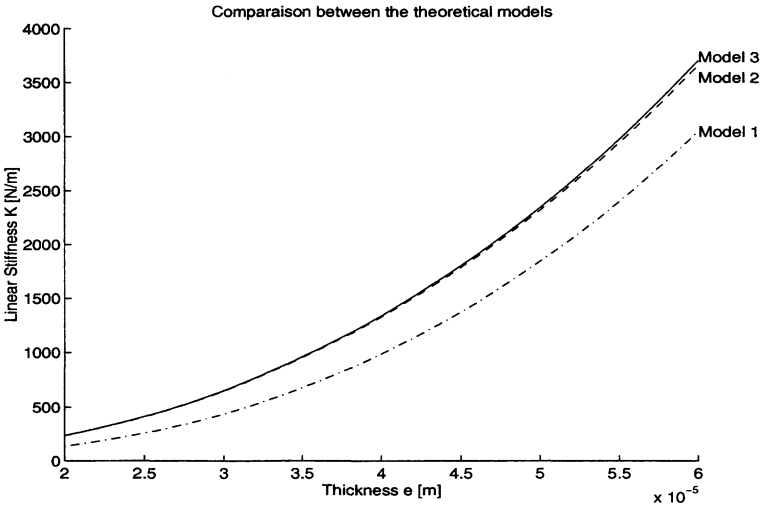

Figure 3 : Linear stiffness K of the parallel spring stage as a function of the thickness of the notch hinges e according to the three models described above. e ranges from 20µm to 50µm. We chose model 3 for the simulation of our small parallel spring stages.

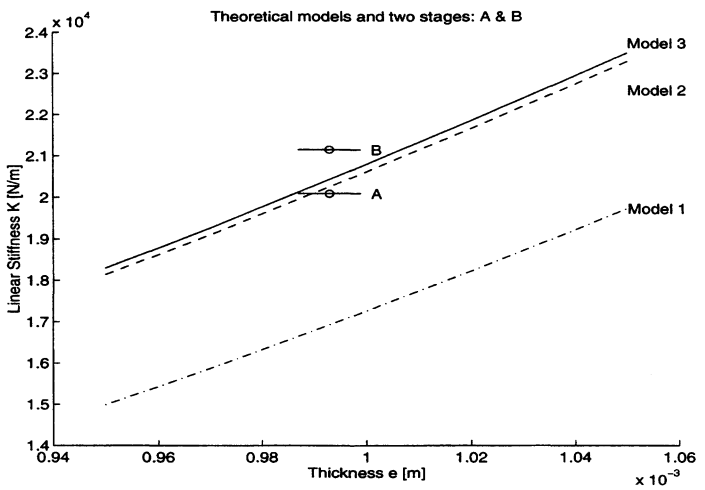

Figure 4 : Comparison between the three models and the measured stiffnesses of two stages (A & B) of large dimensions (e = 993µm). Models 2 and 3 better fit the experimental results. The horizontal bars represent the uncertainty of ±6µm of the measured thickness.

[a] The terms K_{fF} and $K_{\alpha M}$ have been compared to finite element analysis simulations and gave the same values to a precision of approximately 1%. The term $K_{\alpha M}$ is identical to Paros's[20] equation 1.

Model 1 gives stiffnesses lower than models 2 and 3. We do not know where that stems from. Although Smith[2] presents both models 1 and 2, he does not compare them or give any comments on their consistency. We suppose that the factor c is not accurate. To make sure that models 2 and 3 are the closest to physical reality we manufactured by CNC milling two parallel spring stages of large dimensions and measured their stiffnesses (fig. 4) : r = 10mm, l = 50mm, b = 8mm, E = 0.72 10^{11}N/m^2 (Perunal aluminium) and e = 993µm ±6µm. We chose a large thickness e for it to be as independent of machining tolerances as possible[a]. The two stages are identical, barring the manufacturing tolerances. We measured a linear stiffness of 20.09N/mm for the first (stage A) and 21.15N/mm for the second (stage B) while model 1 predicts 16.93N/mm, model 2 predicts 20.25N/mm and model 3 predicts 20.43N/mm. Models 2 and 3 agree better with the measures : the measured stiffnesses are within ±4% of the values predicted by models 2 and 3 and more than 18% away from model 1. We therefore decided to abandon model 1.

It can be clearly seen that models 2 and 3 agree very well over the whole range of thicknesses of our small stages (fig. 3). Their slight difference can be explained by the fact that model 2 assumes the circular flexure hinges to be ideal pivots whereas model 3 considers the joints as bending beams. Since model 3 is closer to physical reality, it is the one we chose for our simulations.

4. WIRE-ELECTRO DISCHARGE MACHINING

The structures were manufactured at AGIE SA Losone, on a wire electro-discharge machine (Agiecut 150 HSS+F), with a wire of 50µm. The materials used are

- spring steel DIN 60SiCr7 (n°1.7108), with a Young's modulus of 2.1 10^{11} N/m^2 and a yield stress of 1030 N/mm^2 (stages 1.1 to 3.8)

- Perunal® aluminium DIN AlZnMgCu1.5 (EN AW-7075), with a Young's modulus of 0.72 10^{11} N/m^2 and a yield stress of 480 N/mm^2 (stages 4.1 to 5.3)

The average surface roughness Ra of the necked down section was evaluated by measuring the roughness of test blocks electro-machined in exactly the same manner (same electrical parameters, same number of runs of the wire, etc.)

We manufactured 18 stages of small dimensions : r = 0.6125mm, l = 8mm and b = 5.5mm. 5 stages where made of aluminum and 13 of steel. The thicknesses e range from 22µm to 50µm. The wire-EDM machining parameters have been optimized to achieve a very small surface roughnesses (Ra=0.3µm for the steel and Ra=0.18µm for the aluminum for one main cut and two trim cuts).

5. TEST BED

The linear stiffness was measured using a high precision weighing machine (Mettler Toledo®), with a resolution of 1mg to measure the forces, and an optical proximity sensor (Keyence®) based on laser triangulation with a resolution of 10nm to measure the displacements induced by the forces. The structure is moved by a micrometric motorised axis, capable of making steps as small as 1µm.

The thickness e of the joints was measured on a profilometer projector using a lens magnification of 200. The precision of the measure is not better than ±1µm. This leads to an important uncertainty of the position of the measured points on our graphs. We have transcribed this uncertainty by a horizontal bar ranging 1µm on each side of the points (fig. 5).

Thanks to the high precision sensors used, the uncertainty of the stiffness measure is negligible when compared to the uncertainty of the thickness measure[b]. Thus it is not represented on the graphs.

---

[a] An uncertainty of ±6µm of the measured thickness of a 1mm thick hinge induces an uncertainty of ±1.5% of the linear stiffness a parallel spring stage. An uncertainty of ±1µm of the measured thickness of a 30µm thick joint induces an uncertainty of ±8.5% of the linear stiffness. Therefore, the stiffnesses predicted by the theoretical models will have a much smaller uncertainty for large stages (stage A and B) than for small stages (stages 1.1 to 5.3).

[b] For a measured stiffness of 20N/mm (stages A and B) the uncertainty of the measured stiffness is 10^{-2} N/mm which represents only 0.05% of the measured value. For the small stages the uncertainty of the measured stiffness is less than 0.1% of the measured values.

6. MEASUREMENTS

Stage number	Material & Young's Modulus (Pa)	Number of runs of the wire	*Ra* (µm)	Measured Thickness e_m (µm)	Measured stiffness *Km* (N/m)	Theoretical stiffness *K* (N/m) for a thickness e_m	Relative deviation $d = (Km-K) / K$ (%)
1.1	Steel *E*= *2.1 x* 10^{11}	1 cut	0.82	31	715	1111	-36 %
1.2				42	2023	2379	-15 %
2.1		2 (1 main cut + 1 trim cut)	0.6	22	218	470	-54 %
2.2				24	321	585	-45 %
2.3				50	3006	3684	-18 %
3.1		3 (1 main cut + 2 trim cuts)	0.3	20	252	370	-32 %
3.2				25	687	647	+6 %
3.3				28	654	861	-24 %
3.4				30	1089	989	+10 %
3.5				31	724	1111	-35 %
3.6				37	1289	1779	-27 %
3.7				41	1981	2240	-12 %
3.8				50	3440	3684	-7 %
4.1	Alumin ium *E*= *0.72 x* 10^{11}	1 cut	1	22	103	161	-36 %
4.2				50	1043	1247	-16 %
5.1		3 (1 main cut + 2 trim cuts)	0.18	27	253	269	-6 %
5.2				34	463	467	-1 %
5.3				45	985	969	+2 %

Table 1 : Characteristics of each of the 18 stages we have machined and measured. For all the stages r = 0.6125mm, l = 8mm and b = 5.5mm.

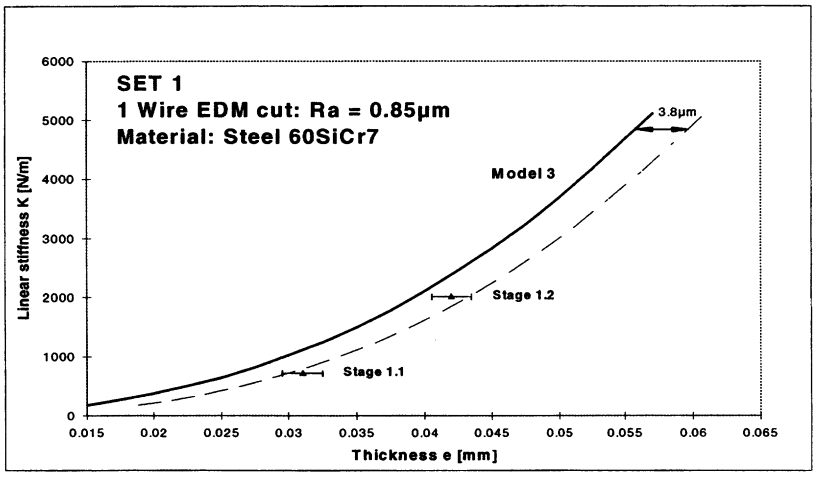

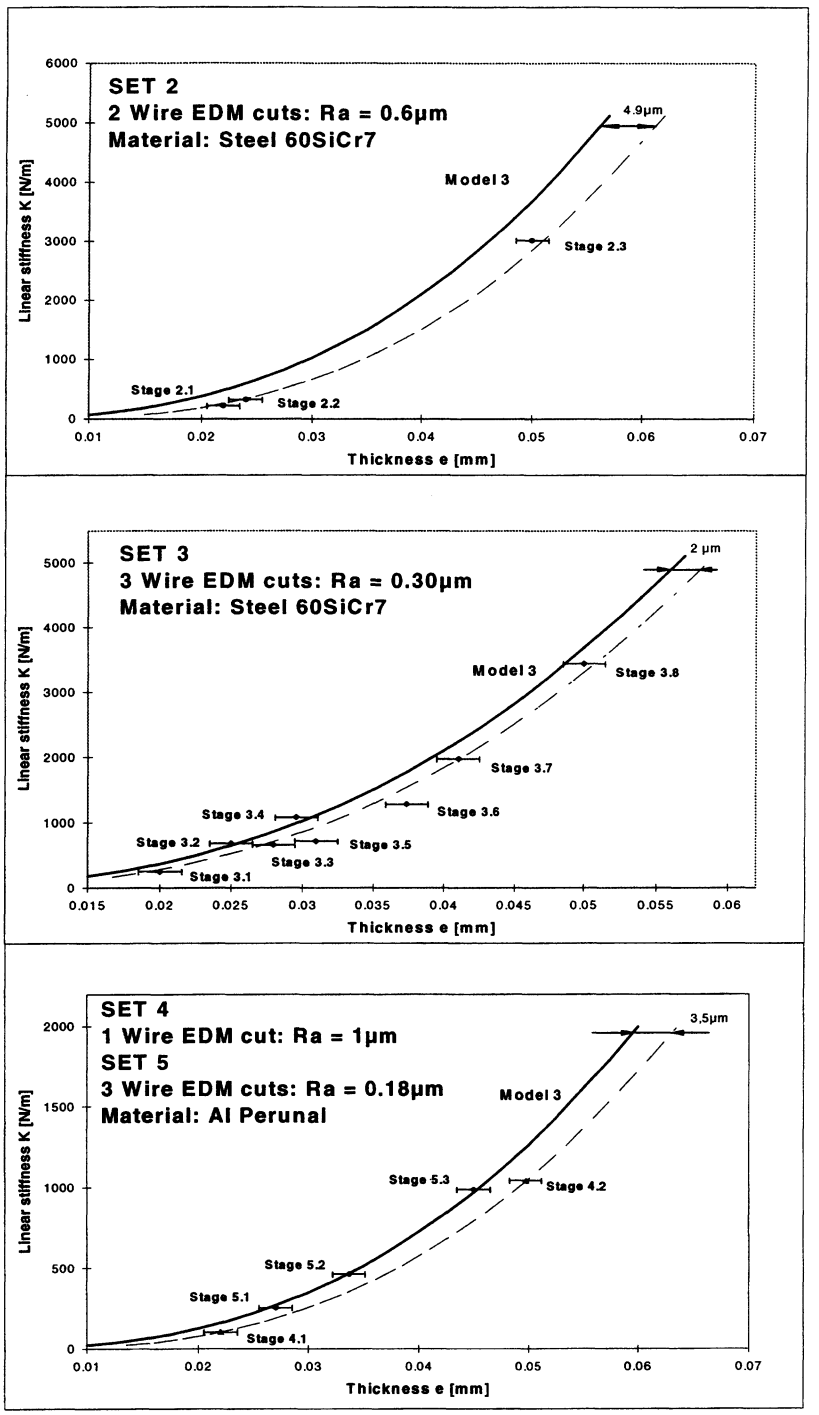

Figure 5 : Comparison of the measured stiffnesses of the parallel spring stages with the theoretical model. The solid curves represent the theoretical model (model 3). The dashed curves are the horizontal translations of the theoretical curves which best fits the measured points. The horizontal bars represent the uncertainty of the measured thickness e of the stages' necks. The stages are sorted in sets of stages of the same roughness.

7. RESULTS

7.1 Observations

To analyse the results we calculated the relative deviation of the measured stiffnesses *Km* from the theoretical stiffnesses *K* predicted by model 3 for the measured thicknesses e_m. The relative deviation is : $d = (Km-K) / K$. These values are given in the last column of table 1.

For example, stage 1.1 has a stiffness 36% smaller ($d = -36\%$) than predicted by model 3 for $e_m = 31\mu m$.

By looking at the values of *d* in table 1 we see that most of these small stages are a lot less stiff than what is predicted theoretically (20% less on average). This was not the case with the two stages of large dimensions A and B which were only a few percent away from the theoretical curve (stage A : 1.7% below, and stage B : 3.5% above). Thus, the theoretical model which is accurate for stages of large dimensions, seems much less valid for stages having necks with very small cross-sections.

7.2 The "neutral zone", a key for analysis

This observation has lead us to put forward the idea that only a fraction of the measured thickness was playing a mechanical role in the bending of the small flexures[22]. As if a thin layer on each side of the necks had been modified by the wire-EDM process and had become "mechanically neutral." We made the hypothesis that this "*neutral zone*" was the cause of the deviation of the measured points from the theoretical model. The thickness of this "neutral zone" can easily be evaluated : for each stage we calculated the theoretical thickness e_{th} which gives (with model 3) a stiffness *K* equal to the measured stiffness *Km* of the stages. The difference between the measured thickness e_m and the theoretical thickness e_{th} represents the part of the joint's section which plays no mechanical role : the "*Neutral Zone*" ($NZ = e_m - e_{th}$).

If this interpretation is pertinent then once we will be able to predict the thickness of the "neutral zone", we will also be able to accurately predict the stiffness of flexures with thin cross-sections : if for a given stage e_m and *NZ* are known, then e_{th} can be deducted and the stiffness can be calculated correctly by the theoretical model.

7.3 The surface roughness, an indicator predicting the "neutral zone" ?

Since we believe that the "neutral zone" is related to surface modifications due to the wire-EDM process, we looked for parameters which characterise the surface quality. We thought of the average surface roughness *Ra* as a good indicator of the surface finishing. Thus we made the hypothesis that *NZ* depends upon Ra and only upon Ra. To test it we sorted the stages in sets of stages of same roughness and plotted for each set a graph of stiffness as a function of thickness (fig. 5). If the hypothesis is correct, then for each set the points should follow a curve (dashed on the graphs) which is a horizontal translation of model 3 (the distance of the horizontal translation is the thickness of the "neutral zones" *NZ* of each set).

7.4 Analysis of the results

Sets 1, 2, 4 and 5 agree with the hypothesis we made : taking into account the uncertainty of the thickness measure (horizontal bars on the graphs) all the points of each set fall on curves which are horizontal translations of model 3. For example, the steel stages which have a roughness $Ra=0.6\mu m$ (set 2) behave as if 4.9µm of their joint's sections were not playing any mechanical role[a] while the aluminium stages with $Ra=1\mu m$ (set 4) behave as if 3.5µm where neutral.

With set 3 no horizontal translation of the theoretical curve exists which crosses all the measured points. This indicates that for set 3 the hypothesis is not confirmed. Thus the model of the "neutral zone" depending only upon roughness is either wrong or incomplete.

7.5 Interpretation

We believe that our model is not wrong but incomplete : we think that there is a "neutral zone" and that its thickness is correlated to roughness but not only to roughness. The influence of other physical properties of the machined surfaces could

[a] It is interesting to note that the maximum peak-to-valley height *Rmax* of the surface profile of the joints of set 2 was measured to be 5.6µm. This roughness, which is present on both sides of the joints, represents an important fraction of the joints' cross-section thus the presence of a 4.9µm thick "neutral zone" for these joints appears plausible. The same remark can be made for the other sets.

explain the deviations of the measured points of set 3. We chose Ra as an indicator of the surface quality because it is an easily accessible physical value, but it is not the only parameter which characterises the Wire-EDM machined surface.

The juxtaposition and overlapping of the minute craters due to the individual sparkles during EDM modifies not only the roughness but also the structures of the material just below the surface. One of these modifications is the apparition of an irregular "white layer" which probably influences the joints' behaviour[23,24]. Figure 6 shows a picture of a neck's middle section on which the "white layer" can clearly be seen. It is known that the "white layer" which appears on aluminium after EDM is much thinner than the layer found on steel. This could be a plausible explanation to the fact that the points of set 4 and 5 (stages made of aluminium) fluctuate much less than that of the other sets : since the "white layer" is very uneven, the thicker it is, the less predictable will be the stiffness of the joints.

The layer making the junction between the "white layer" and the bulk material also has its structure and its hardness modified by the high thermal stresses it endures during the sparkling process. This layer called "thermally affected zone[24]" or "transformation zone[23]" might influence mechanically the flexures.

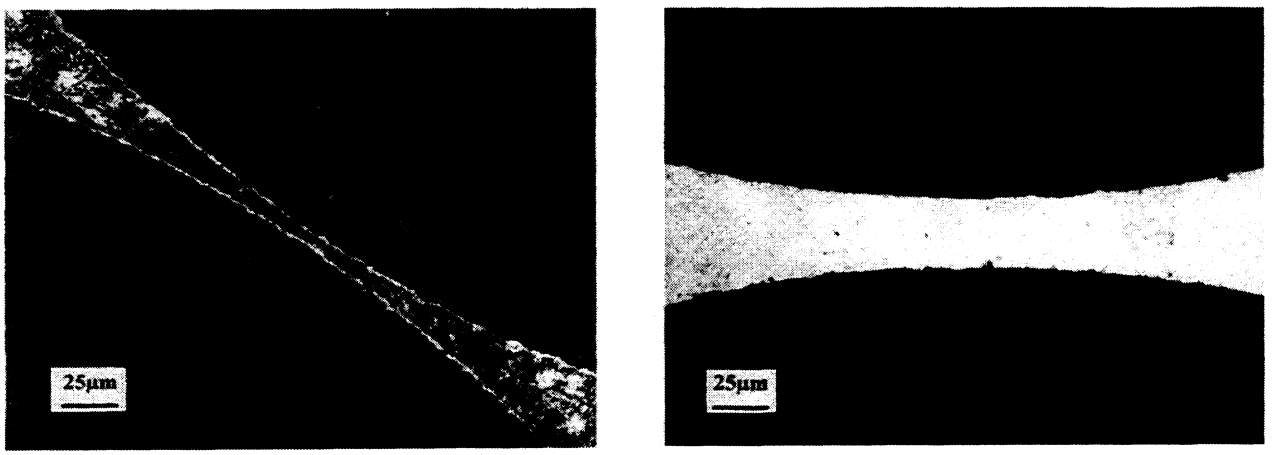

Figure 6 :

Left : Picture of the middle section of a notch hinge made of steel (DIN 60SiCr7). The "white layer" can clearly be seen on both sides of the joint. This joint is 8µm thick. It was wire-EDM machined with one main cut and two trim cuts. Its roughness is Ra=0.73µm. The piece was polished and then etched with picric acid to reveal clearly the "white layer" which has been evaluated to vary between 1µm and 2.5µm

Right : Notch hinge made of Perunal Aluminium (DIN AlZnMgCu1.5). The joint is 34µm thick. It was wire-EDM machined with one main cut and two trim cuts. Its roughness is Ra=0.18µm. Although the piece was polished and etched like the steel piece, no "white layer" can be seen on its surfaces.

8. CONCLUSION

8.1 Process

Theoretical modelling : We described three theoretical models for the calculation of the linear stiffness of the parallel spring stage. We chose the model which best suited the experimental measurements made on stages whose geometrical dimensions are known with a great degree of accuracy (stages A and B).

Observation : Then we made the observation that this model which is valid for stages of large dimensions produces large errors for stages with necks of very small cross-section machined by wire-EDM.

Explicative hypothesis : Trying to find an explanation to this observation, we made the hypothesis that on the surface of each neck a thin layer affected by the EDM process was not playing any mechanical role in the flexure and that the thickness of this layer is related to the roughness of the surface.

Experimental testing of the hypothesis : We measured the stiffnesses of 18 stages made of steel and aluminium of different joint thicknesses (20µm to 50µm) and different joint roughnesses (*Ra* = 0.18µm to 1µm).

8.2 Conclusions

- The classical theoretical model can produce errors greater than 50% of the measured value (stage 2.1) when applied to stages of small dimensions.

- The hypothesis of the existence of a "neutral zone" which depends only upon the surface roughness of the joints is corroborated by most of the experimental results and especially by the aluminium stages (sets 4 and 5).

- The fact that one of the measured sets of stages (set 3) does not verify the hypothesis indicates that although roughness is a major factor affecting the "neutral zone" it is probably not the only one. The idea of the thickness of the "white layer" being another factor has been put forward.

- The stages made of Perunal aluminium have a behaviour which is much more predictable than the stages made of steel 60SiCr7. We have attributed this phenomenon to the "white layer" which is much thinner with aluminium than steel.

- The important fluctuations observed for stages 3.1 to 3.6 are a sign of the poorly predictable behaviour of the steel 60SiCr7 flexures of very small cross-sections. Again this could be the result of a thick and irregular "white layer" on the joints. It could also be the consequence of the non-homogeneity of the material's microstructure : a metallographic analysis of the steel 60SiCr7 has shown numerous inclusions of impurities of rather large dimensions (tens to hundreds of microns). The use of a more homogenous steel[25] made from powder metallurgy like the steel DIN 1.2380 (X220CrVMo13-4) could produce more predictable results. This is an issue to be investigated.

So far, we have applied the "theory of the neutral zone" only to parallel spring stages but there are great chances that all what has been said in this paper is also applicable to other types of flexures of very small dimensions fabricated in the same manner. Hence we hope to be able to generalise the results of this study to all the wire-EDM machined flexible structures. This will be of great interest when designing complex flexures for long strokes which need flexible parts of ever thinner cross-sections.

ACKNOWLEDGMENTS

The authors are grateful to I. Paganetti and H. Gruber from AGIE for their support for the electro-discharge machining of the stages and to P. Ziegler from AGIE for the metallographic analysis of the joints. They also wish to thank C. Aymon from the Swiss Federal Institute of Technology of Lausanne for his help during the stiffness measurements of the stages.

REFERENCES

1. E. Pernette, S. Henein, I. Magnani, & R. Clavel, "Design of parallel robots in microrobotics", *Robotica*, Vol 15, pp. 417-420, UK : Cambgrige University Press, 1997
2. S.T. Smith & D.G. Chetwynd, *Foundations of ultraprecision mechanism design. Developments in nanotechnology*, Vol. 2, Chap. 4 : "Flexure design for positioning and control", pp. 95-129, Series Editor : D. Keith Bowen, University of Warwick, UK, 1992
3. W. Ehrfeld, H. Lehr, F. Michel, A. Wolf, H. Gruber & A. Bertholds, "Micro electro discharge machining as a technology in micromachining", *Proc. SPIE Micromachining and Microfabrication Process Technology II,* Austin Texas, 14-15 October 1996
4. S. Clay, "The mechanical development of the microscope. A new fine-adjustment", *Journ. of the Royal Microscopical Society, Transactions of the society*, PI. I., pp. 1-7, 1937
5. R. V. Jones & I. R.Young, "Some parasitic deflexions in parallel spring movements", *J. sci. Instrum.*, 33, pp. 11-15, 1956
6. J. E. Plainevaux, *Nuovo Cimento*, **10**,1953
7. J. E. Plainevaux, "Guidage rectiligne sur lames élastiques. Comparaison de divers types connus et nouveaux", *Nuovo Cimento*, **12**, pp. 37- 47, 1954
8. Y. Muranaka, M. Inaba, T. Asano & E. Furukawa, "Parasitic rotations in parallel spring movements", *Int. J. Japan Soc. Prec. Eng.*, Vol 25, No. 3, pp. 208-213,1991
9. A. Kyusojin & D. Sagawa, "Development of linear and rotary movement mechanism by using flexible strips", *Bull. Japan Soc. of Prec. Engg.*, Vol. 22, No. 4, pp. 309-314, 1988
10. J. E. Plainevaux, "Mouvement parasite vertical d'une suspension élastique symétrique à compensation et asservissement", *Nuovo Cimento*, **11**, pp. 626-637, 1954

11. R. V. Jones, "Some use of elasticity in instrument design", *J. sci. Instrum.*, vol. 39, pp. 193-203, 1962
12. R. V. Jones, "Parallel and rectilinear spring movements", *J. sci. Instrum.*, 28, pp. 38-41, 1951
13. S.T. Smith, D.G. Chetwynd & D.K. Bowen, "Design and assessment of high precision monolithic translation mechanisms", *J. Phys. E: Sci. Instrum.*, 20, pp. 977-983, 1987
14. P. Genequand & P. Schwab, "Micro-aligneur pour composants d'optique guidée monomode", *Proc. SSC-ASMT-85, 59ème congrès, Interlaken, Switzerland*, pp. 79-82,1985
15. P. Schwab, T. Edye & P.M. Genequand, "0.01 micron resolution fibre optic positionning stage", *SPIE Vol. 1014 Micro-Optics*, Centre Suisse d'Electronique et de Microtechnique S.A.- Recherche et Développement - Maladière 71, 2000 Neuchâtel 7, Switzerland, 1988
16. M. Alemanni, G. Mana, G. Pedrotti, P.P. Strona, & G. Zosi , "On the construction of a zerodur translation device for x-ray interferometer scanning", *Metrologia.* Vol. 22, pp.55-63, 1986
17. U. Kuetgens, P. Becker, G. Bertolotto Binac, V. Jäger, J. Stümpel & G. Zosi, "FEM study of a monolithic silicon translation mechanisms for a 10 µm scanning x-ray interferometer", *Proc. of the 3rd Int. Conf. on Ultraprecsion Manufacturing in Engineering*, Aachen, Germany, May 1994
18. A. Dettmer, V. Jäger & U. Kuetgens, "Machining of a monolithic silicon x-ray interferometer - a challenge for manufacturing", *Proc. of 8th Int. Precision Engineering Seminar,* Compiègne, France May 1995
19. T. Katoh, N. Tsuda & M. Sawabe, "One piece compound parallel spring with reduction flexure levers", *Bull. Japan Soc. of Prec. Engg.*, Vol. 18, No. 4, pp. 329-334, 1984
20. J. M. Paros & L. Weisbord, "How to design flexure hinges", *Machine design,* November 25, pp. 151-156, USA: Little Falls, N. J., 1965
21. J.M. Gere & S. P. Timoshenko, *Mechanics of materials*, Third edition, pp. 461-465, PWS-KENT Publishing Company, Boston, 1990
22. S. Henein, S. Bottinelli, R. Clavel & A. Hodac, "Wire electro-discharge machined parallel spring stages for microrobotics", *Proc. of the 9thInt. Precision Engineering Seminar and the 4th Int. Conf. on Ultraprecsion in Manufacturing Engineering*, pp. 448-451, Braunschweig , Germany, 1997
23. F.-J. Sendler, "Extending die life with planetary EDM", *AGIE experience of the best*, n°9, pp. 13-15, AGIE, CH-6616 Losone, January 1996
24. L. Bianchi & E. Rigal, "Usinage par électro-érosion", *Techniques de l'ingénieur*, vol. B7, pp. B7310-1 to B7310-23, Paris : Istra, 1987
25. P. Ziegler, "Necessary conditions for programmable EDM results", *AGIE experience of the best*, n°7, pp. 8-12, AGIE, CH-6616 Losone, May 1995